Ulysses mission-long observations of radial IMF in solar wind rarefaction regions

D. Lario and E.C. Roelof
The Johns Hopkins University. Applied Physics Laboratory

ACE/SOHO/STEREO/Wind Workshop
Kennebunkport, ME 8-10 June 2010

Reference: *Proceedings Solar Wind 12,* ***AIP***, 2010

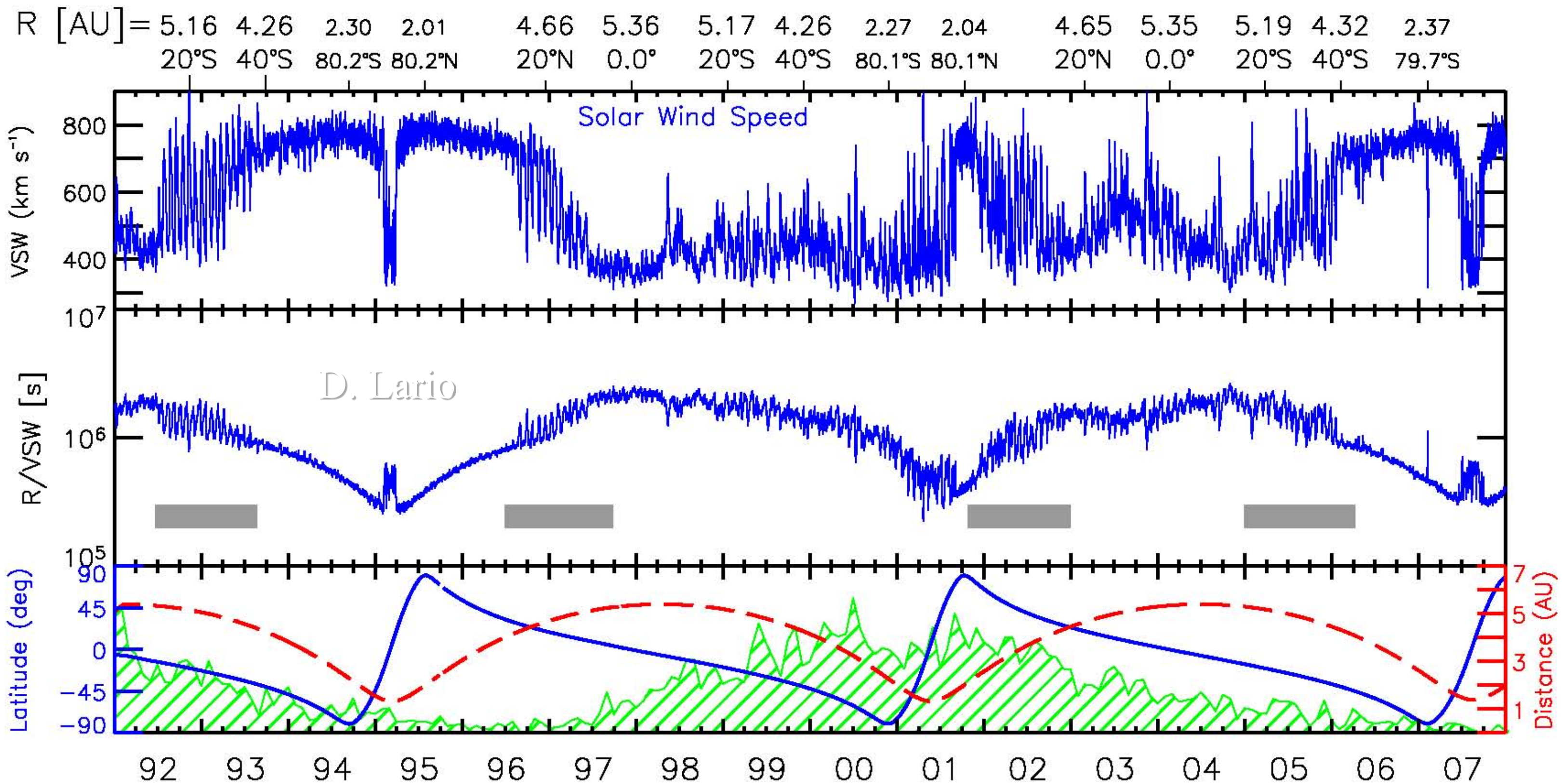

R [AU]= 5.16 4.26 2.30 2.01 4.66 5.36 5.17 4.26 2.27 2.04 4.65 5.35 5.19 4.32 2.37
20°S 40°S 80.2°S 80.2°N 20°N 0.0° 20°S 40°S 80.1°S 80.1°N 20°N 0.0° 20°S 40°S 79.7°S
Solar Wind Speed
VSW (km s⁻¹)
800
600
400
10⁷
10⁶
10⁵
R/VSW [s]
D. Lario
Latitude (deg)
90
45
0
−45
−90
Distance (AU)
7
5
3
1
92 93 94 95 96 97 98 99 00 01 02 03 04 05 06 07

Extrapolation back to the Sun using the observed Solar Wind velocity: dwells

A solar wind parcel observed at heliocentric distance R and longitude ϕ at time t was at the source surface at R_0, ϕ_0 at time t_0.
Let τ be the transit time from source surface to the spacecraft.

$$\left.\begin{aligned} R_0 &= R - V(t)\tau \\ \phi_0 &= \phi - \Omega_\odot \tau \end{aligned}\right\}$$

$$\tau = \frac{\phi - \phi_0}{\Omega_\odot} = \frac{R - R_0}{V(t)} = t - t_0$$

$$\frac{R}{V(t)} \approx t - t_0$$

Roelof and Krimigis [1973]

Plotting R/V as a function of time, we can identify a characteristic solar wind structure, the **"dwell"** in which the longitude $\phi_0(t)$ remains approximately the same.
In a R/V versus time , **"dwells"** show up as straight lines with slope equal to one.

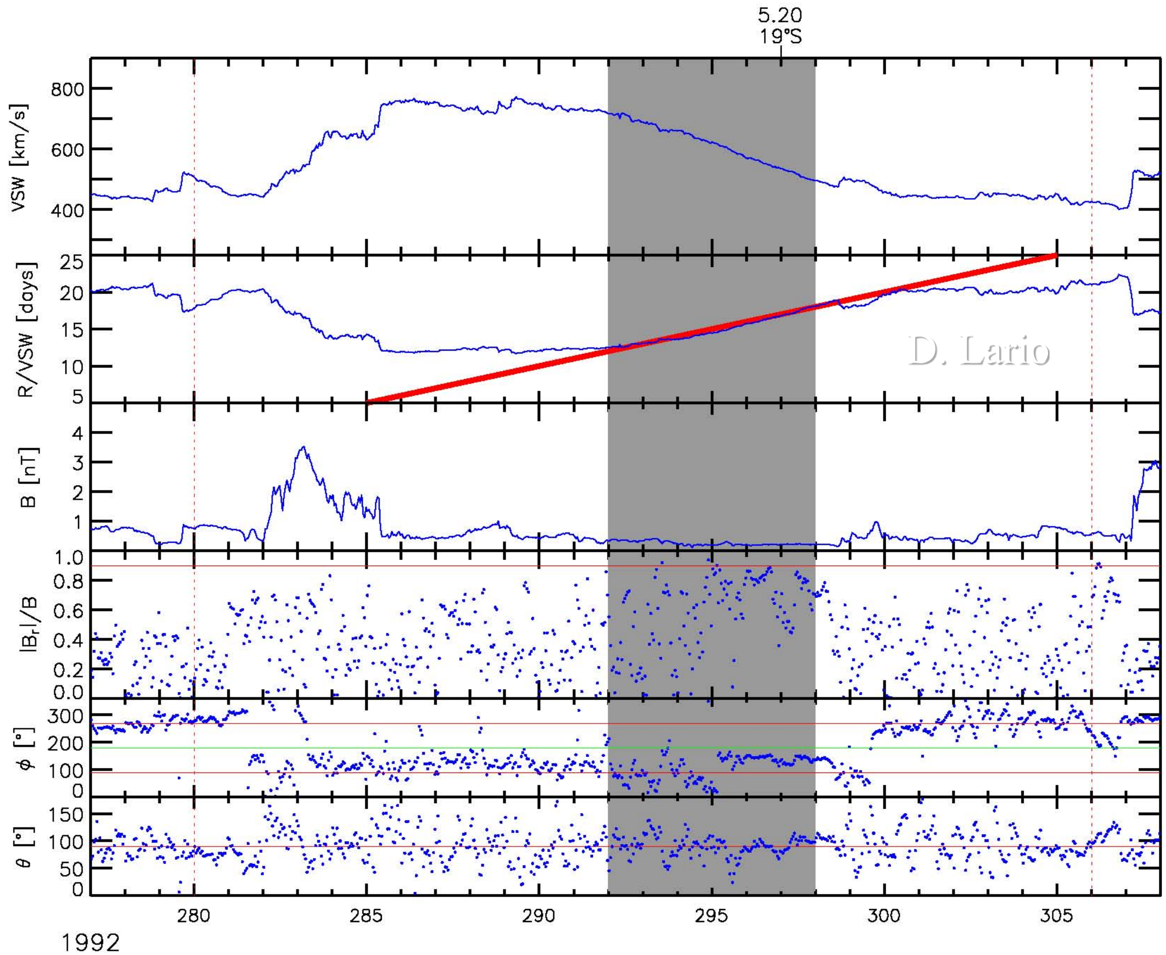

cos(α)=B_r/B

At 4-5 AU→cos(α)~0.25

for Parker field

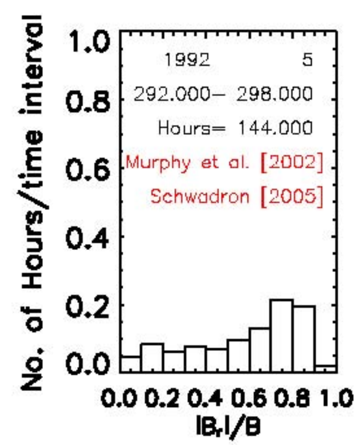

Murphy et al. [2002]

Schwadron and McComas [2005]

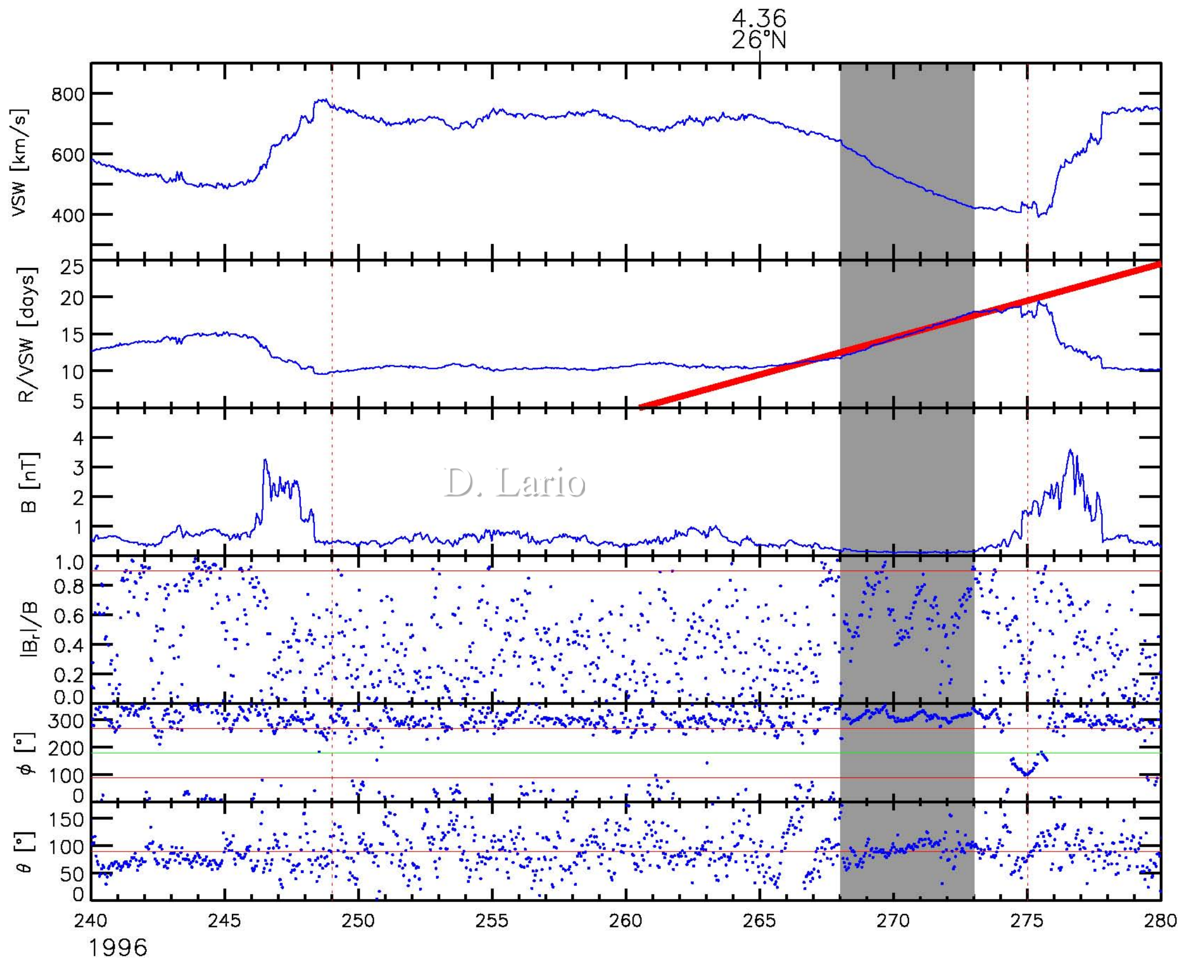

cos(α)=B_r/B

At 4-5 AU→cos(α)~0.25

for Parker field

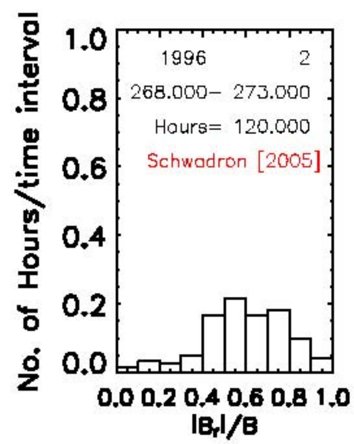

Smith et al. [2000]

Schwadron and McComas [2005]

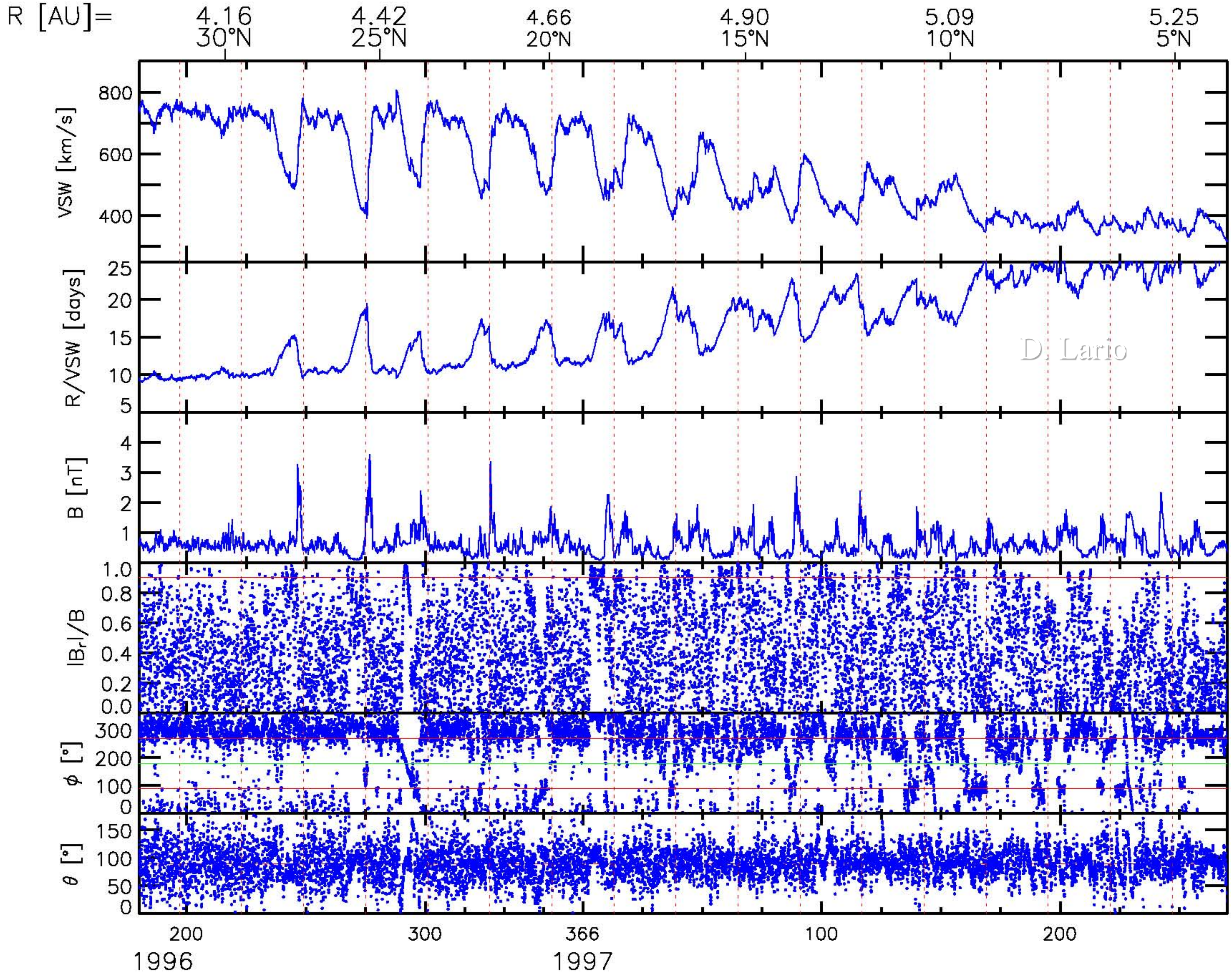

R [AU]=
4.16
30°N
4.42
25°N
4.66
20°N
4.90
15°N
5.09
10°N
5.25
5°N
VSW [km/s]
800
600
400
R/VSW [days]
25
20
15
10
5
D. Lario
B [nT]
4
3
2
1
$|B_r|/B$
1.0
0.8
0.6
0.4
0.2
0.0
ϕ [°]
300
200
100
0
θ [°]
150
100
50
0
200
300
366
100
200
1996
1997

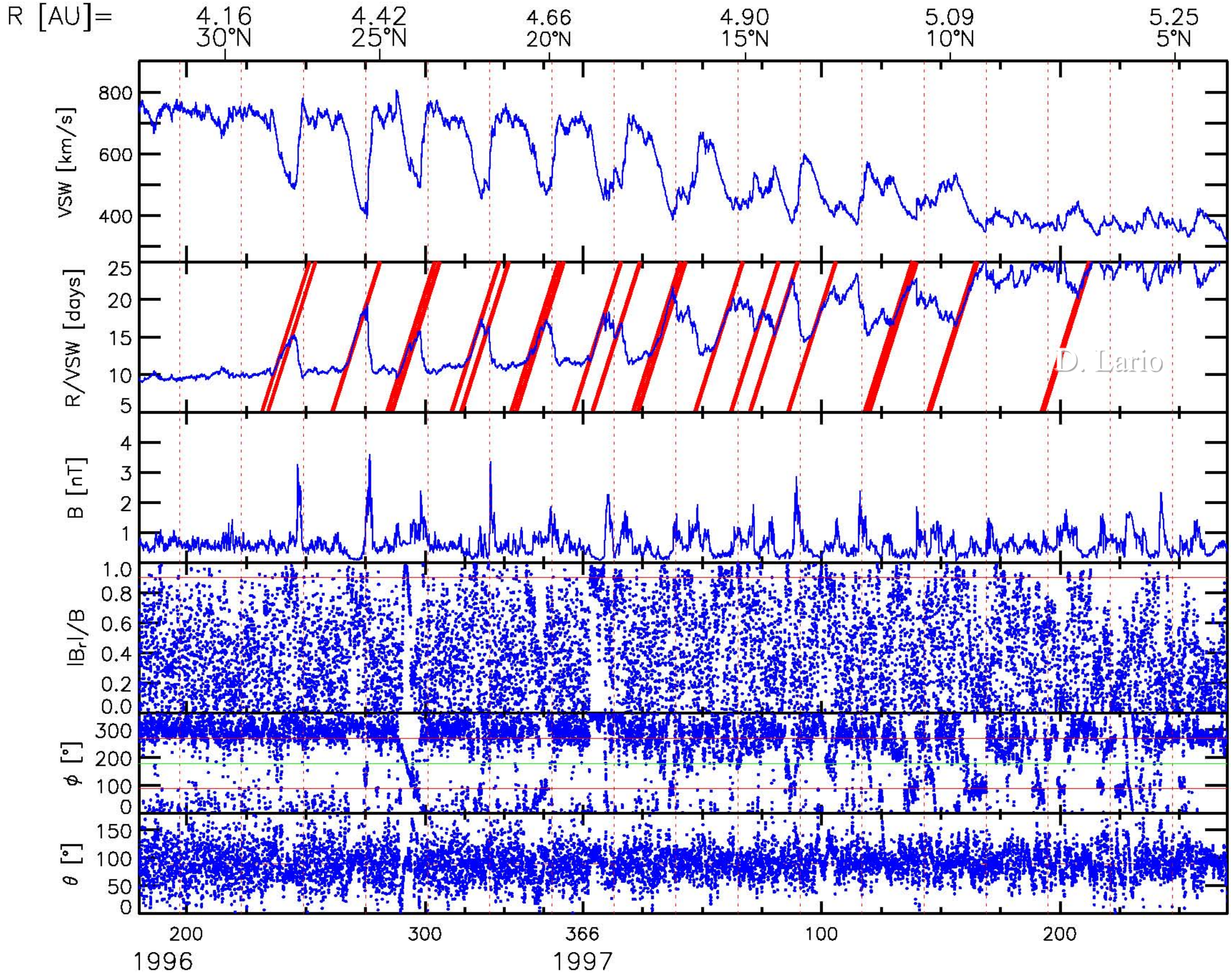

R [AU]=
4.16
30°N
4.42
25°N
4.66
20°N
4.90
15°N
5.09
10°N
5.25
5°N
VSW [km/s]
R/VSW [days]
B [nT]
|B_r|/B
φ [°]
θ [°]
D. Lario
200
300
366
100
200
1996
1997

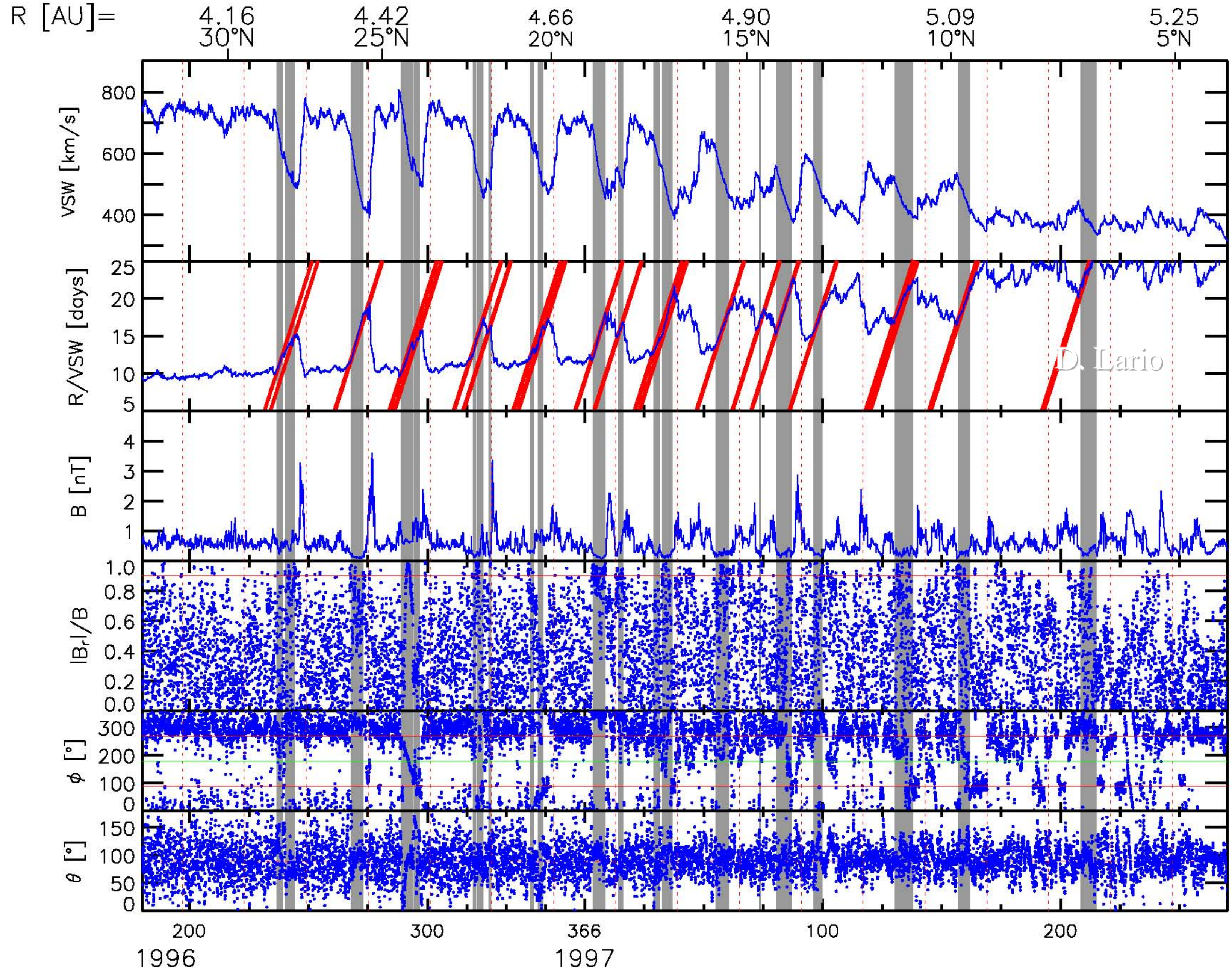
R [AU]=
4.16
30°N
4.42
25°N
4.66
20°N
4.90
15°N
5.09
10°N
5.25
5°N
VSW [km/s]
800
600
400
R/VSW [days]
25
20
15
10
5
D. Lario
B [nT]
4
3
2
1
|B_r|/B
1.0
0.8
0.6
0.4
0.2
0.0
φ [°]
300
200
100
0
θ [°]
150
100
50
0
200
300
366
100
200
1996
1997

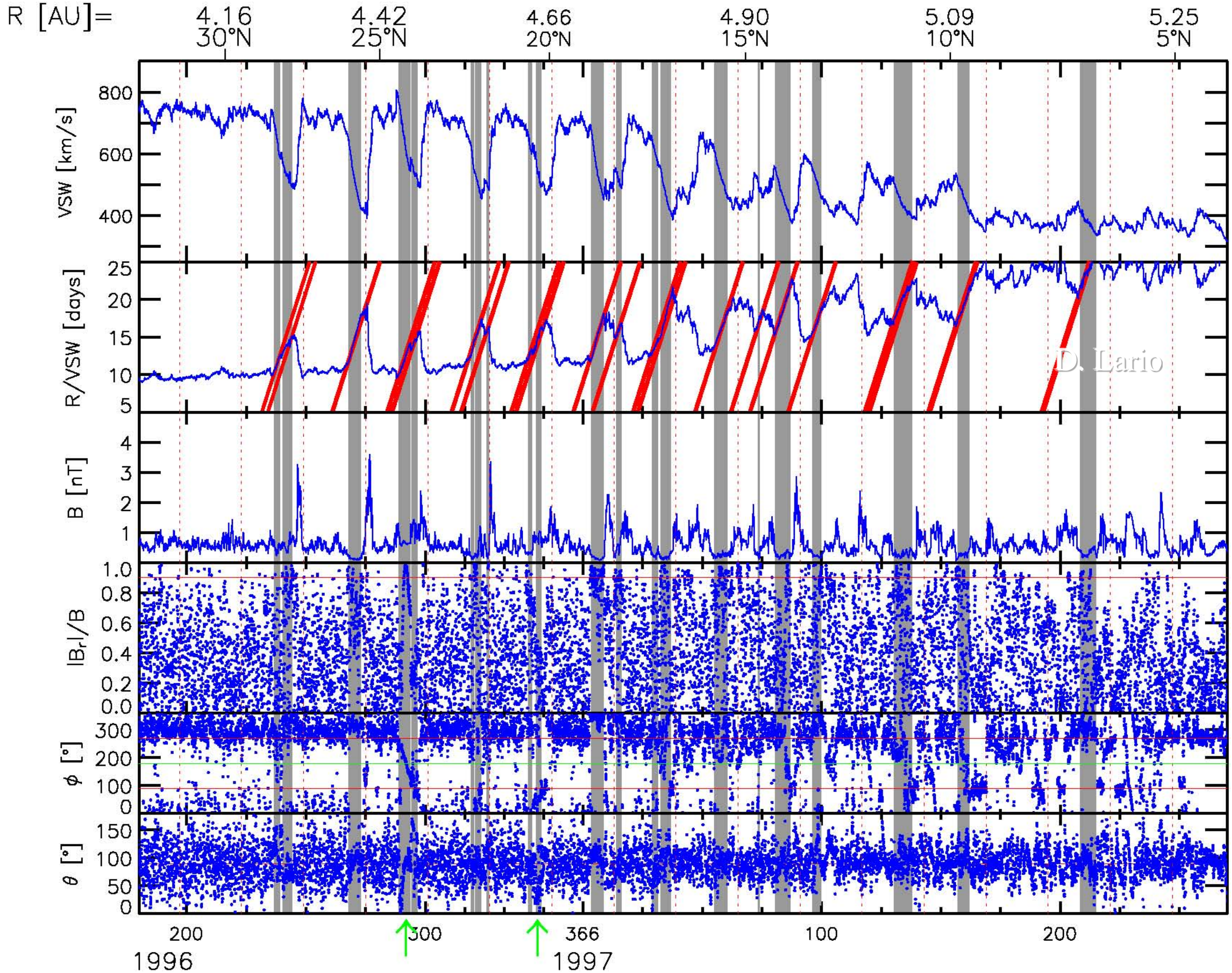

R [AU]=
4.16
30°N
4.42
25°N
4.66
20°N
4.90
15°N
5.09
10°N
5.25
5°N
VSW [km/s]
R/VSW [days]
B [nT]
$|B_r|/B$
ϕ [°]
θ [°]
D. Lario
200
300
366
100
200
1996
1997

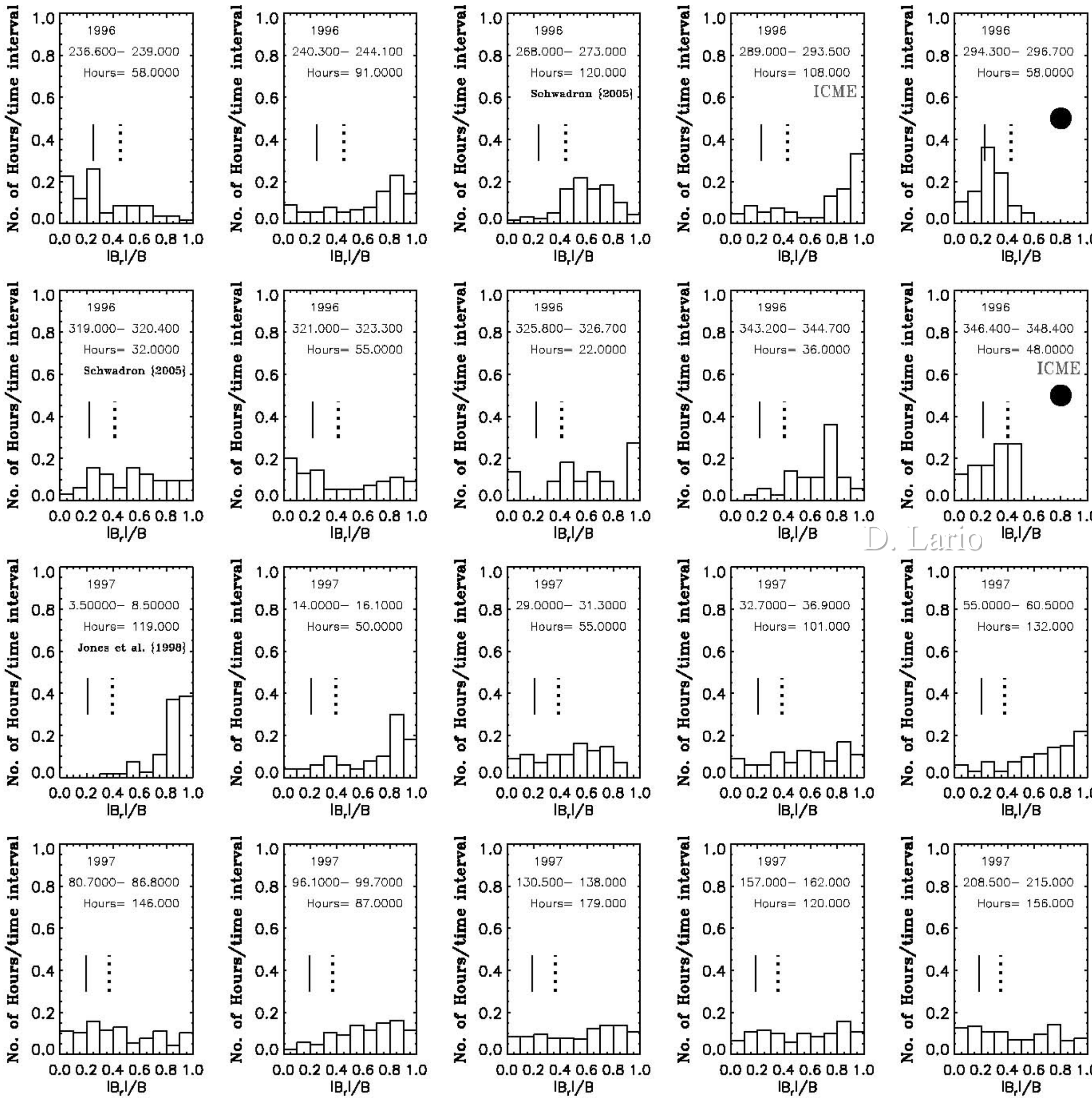
No. of Hours/time interval
|B_r|/B
1996
236.600– 239.000
Hours= 58.0000
1996
240.300– 244.100
Hours= 91.0000
1996
268.000– 273.000
Hours= 120.000
Schwadron (2005)
1996
289.000– 293.500
Hours= 108.000
ICME
1996
294.300– 296.700
Hours= 58.0000
1996
319.000– 320.400
Hours= 32.0000
Schwadron (2005)
1996
321.000– 323.300
Hours= 55.0000
1996
325.800– 326.700
Hours= 22.0000
1996
343.200– 344.700
Hours= 36.0000
1996
346.400– 348.400
Hours= 48.0000
ICME
1997
3.50000– 8.50000
Hours= 119.000
Jones et al. (1998)
1997
14.0000– 16.1000
Hours= 50.0000
1997
29.0000– 31.3000
Hours= 55.0000
1997
32.7000– 36.9000
Hours= 101.000
1997
55.0000– 60.5000
Hours= 132.000
1997
80.7000– 86.8000
Hours= 146.000
1997
96.1000– 99.7000
Hours= 87.0000
1997
130.500– 138.000
Hours= 179.000
1997
157.000– 162.000
Hours= 120.000
1997
208.500– 215.000
Hours= 156.000

96-97

D. Lario

Parker spiral

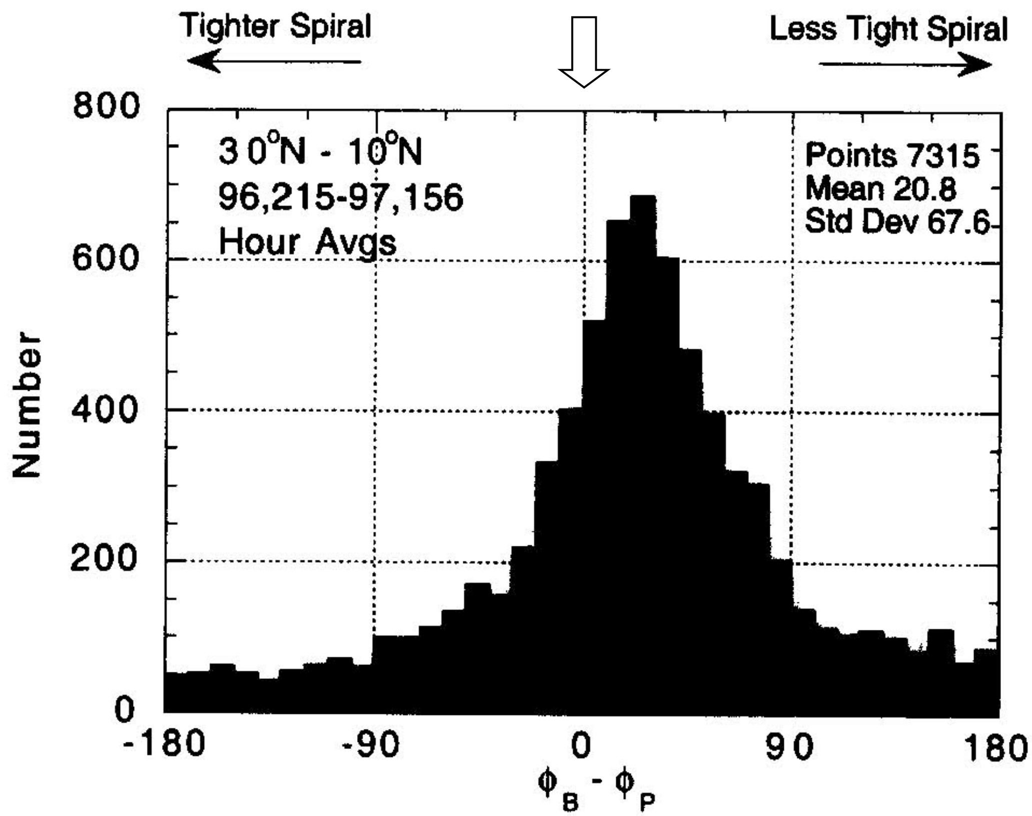

Fig. 3. Histogram of the differences between the observed and Parker spiral angles in the mid-latitude zone (10° - 30°) containing CIRs and CRRs. Both the mean and the most probable values show a substantial departure in the sense of the field direction being more radial than the model predicts. The solar wind speed was used to compute the expected angle.

96-97

Smith et al. [2000]

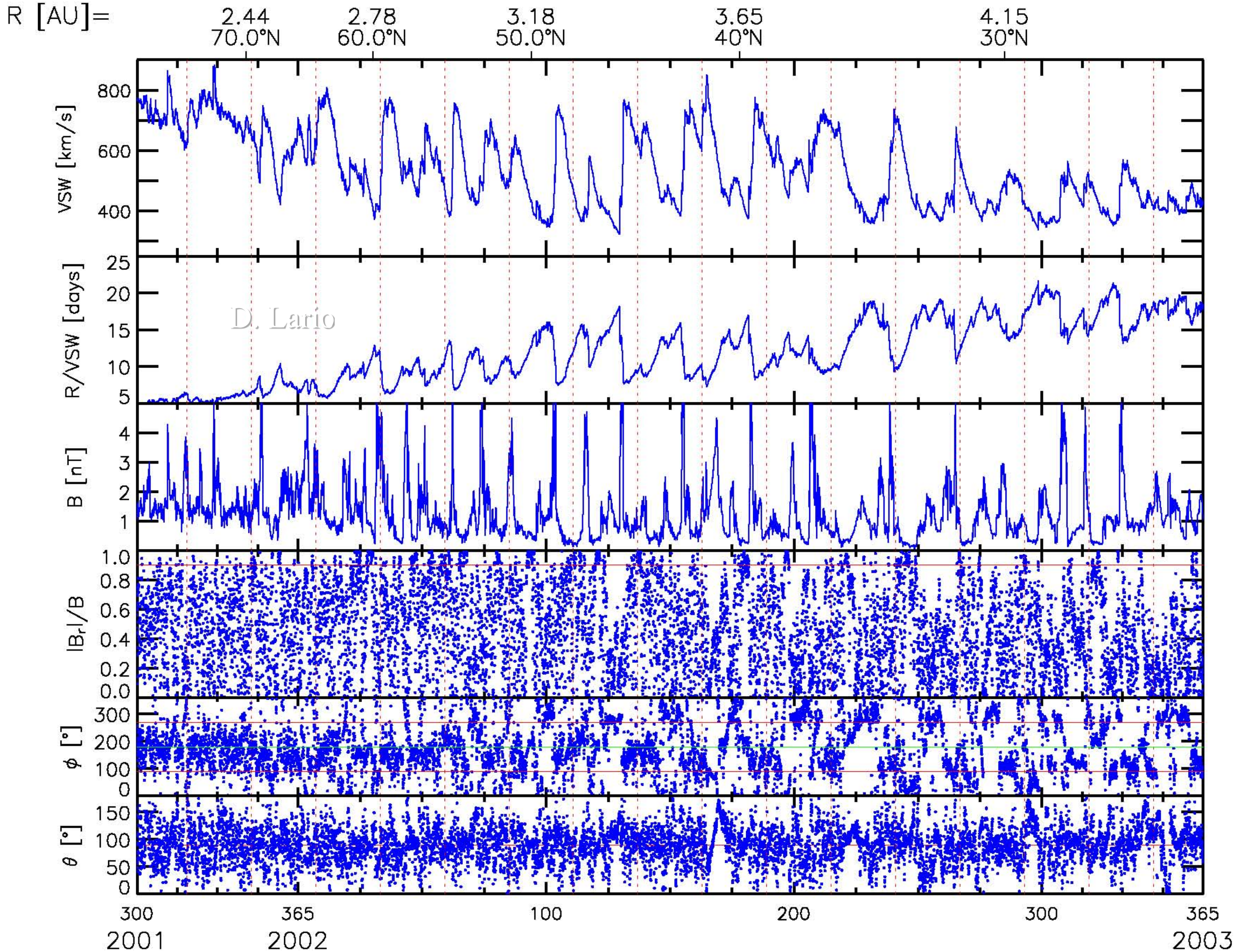

R [AU]=
2.44 70.0°N
2.78 60.0°N
3.18 50.0°N
3.65 40°N
4.15 30°N
VSW [km/s]
R/VSW [days]
D. Lario
B [nT]
|B_r|/B
φ [°]
θ [°]
300
365
100
200
300
365
2001
2002
2003

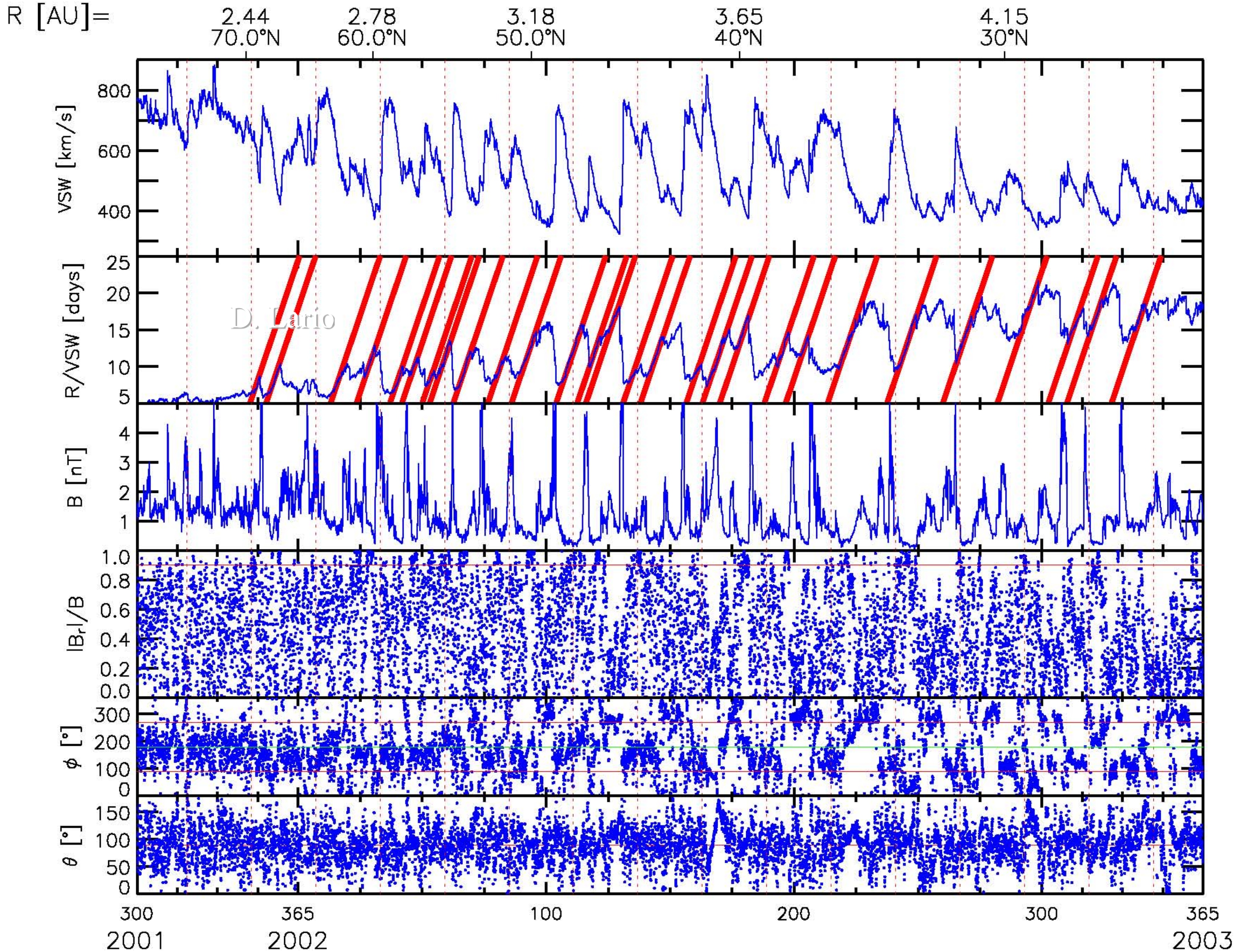

R [AU]=
2.44
70.0°N
2.78
60.0°N
3.18
50.0°N
3.65
40°N
4.15
30°N
VSW [km/s]
800
600
400
R/VSW [days]
25
20
15
10
5
D. Lario
B [nT]
4
3
2
1
|Br|/B
1.0
0.8
0.6
0.4
0.2
0.0
φ [°]
300
200
100
0
θ [°]
150
100
50
0
300
365
100
200
300
365
2001
2002
2003

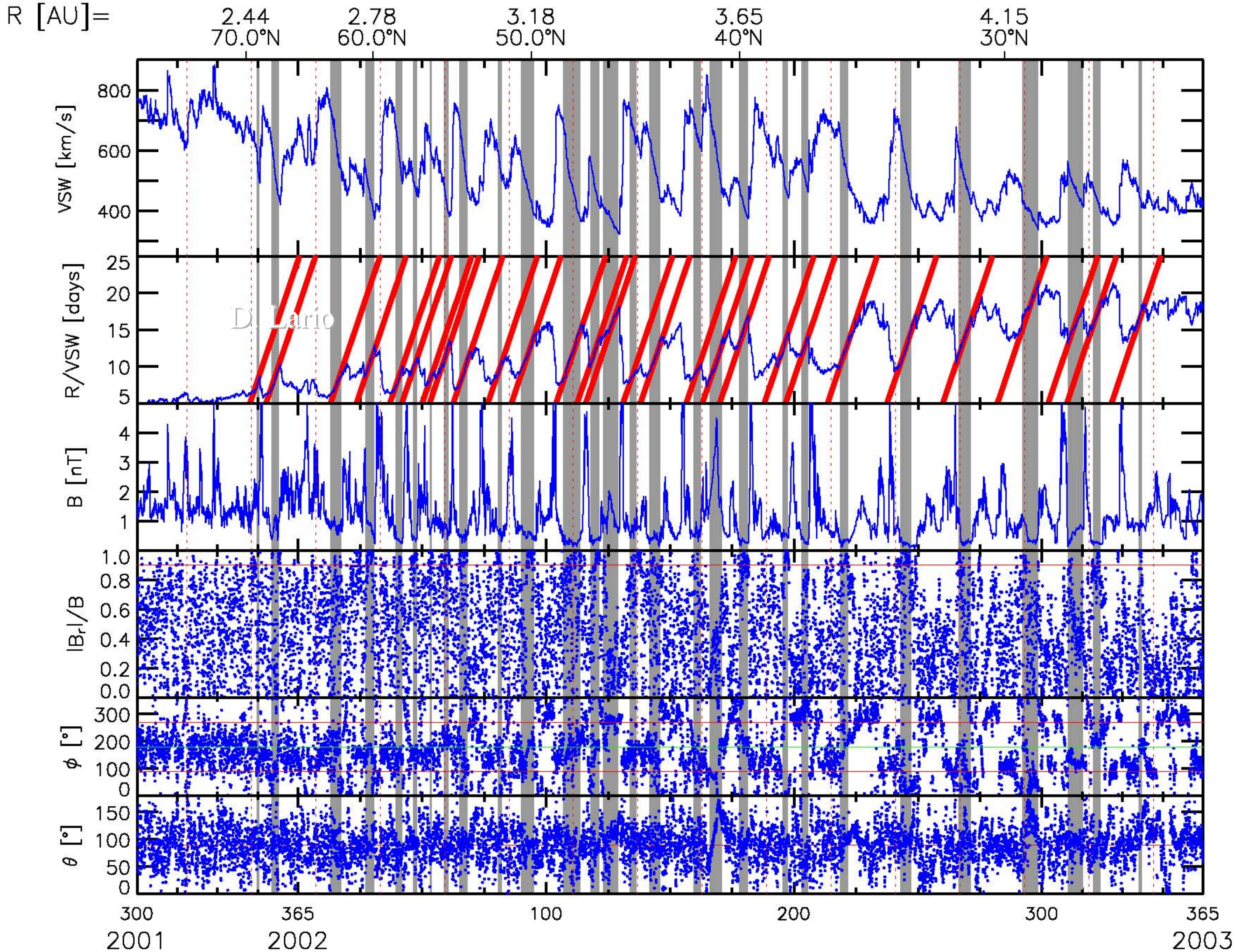

R [AU]=
2.44
70.0°N
2.78
60.0°N
3.18
50.0°N
3.65
40°N
4.15
30°N
VSW [km/s]
R/VSW [days]
D. Lario
B [nT]
|B_r|/B
φ [°]
θ [°]
300
365
100
200
300
365
2001
2002
2003

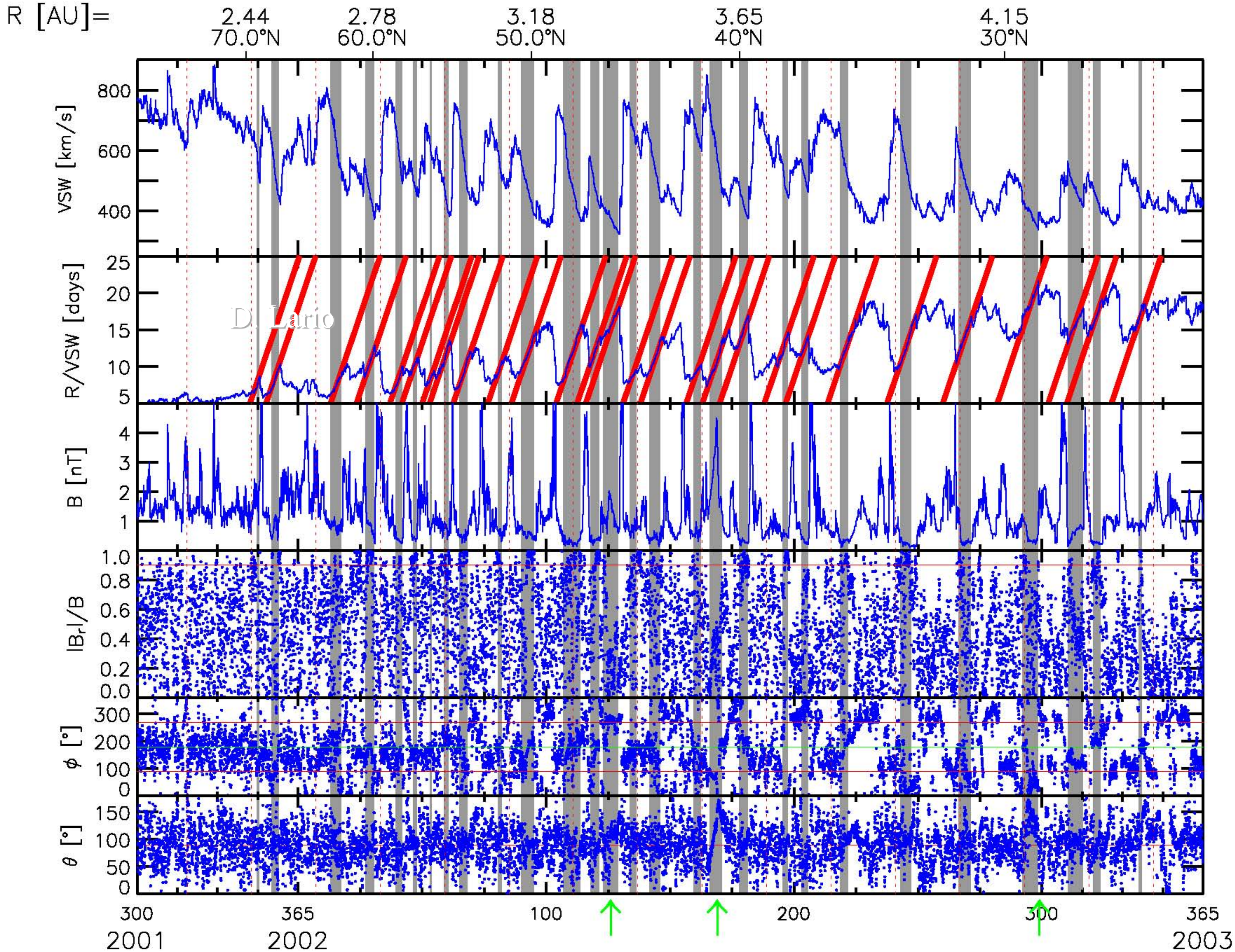

R [AU]=
2.44 70.0°N
2.78 60.0°N
3.18 50.0°N
3.65 40°N
4.15 30°N
VSW [km/s]
R/VSW [days]
D. Lario
B [nT]
|Br|/B
φ [°]
θ [°]
300
365
100
200
300
365
2001
2002
2003

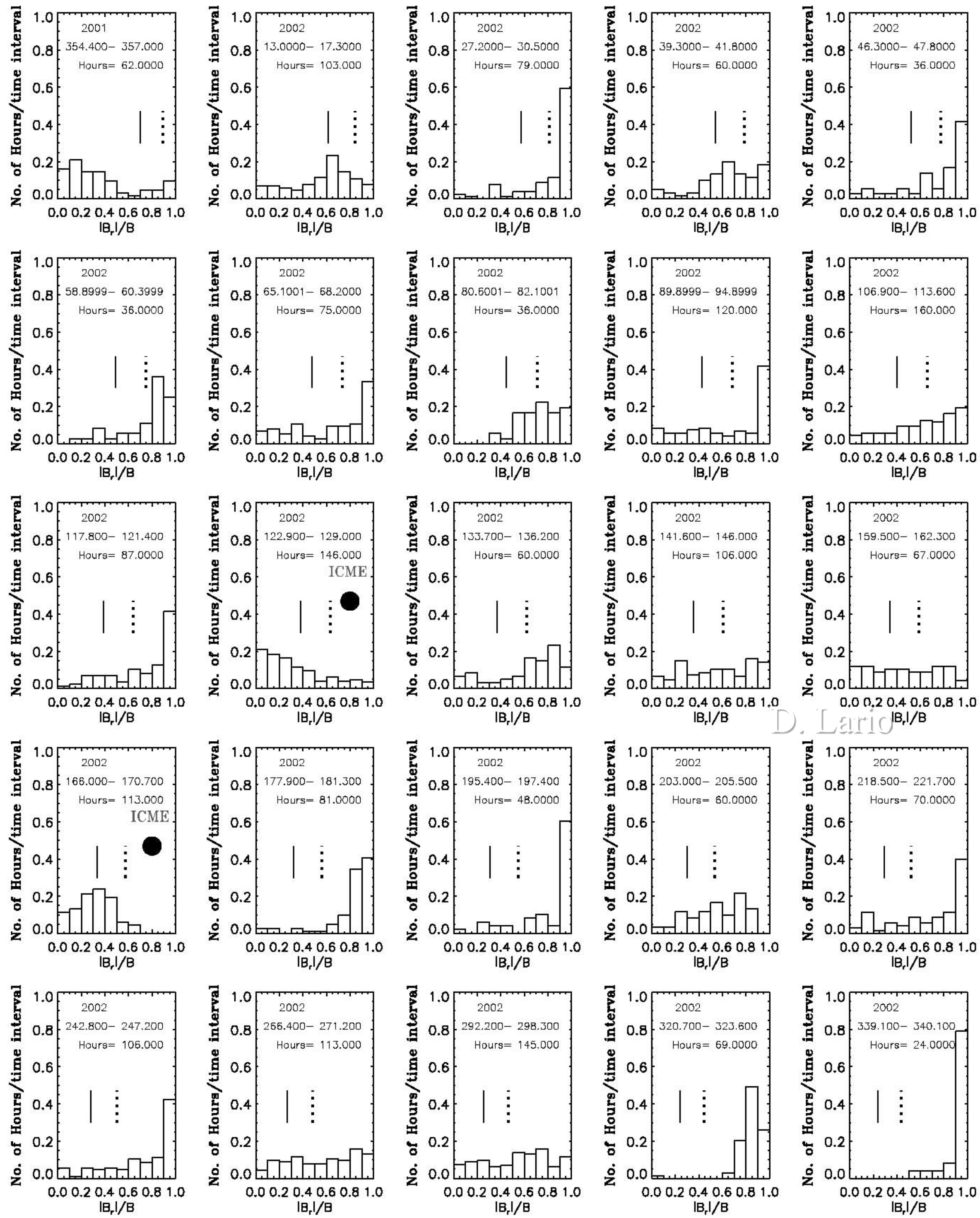
No. of Hours/time interval
|B_r|/B
2001
354.400– 357.000
Hours= 62.0000
2002
13.0000– 17.3000
Hours= 103.000
2002
27.2000– 30.5000
Hours= 79.0000
2002
39.3000– 41.8000
Hours= 60.0000
2002
46.3000– 47.8000
Hours= 36.0000
2002
58.8999– 60.3999
Hours= 36.0000
2002
65.1001– 68.2000
Hours= 75.0000
2002
80.6001– 82.1001
Hours= 36.0000
2002
89.8999– 94.8999
Hours= 120.000
2002
106.900– 113.600
Hours= 160.000
2002
117.800– 121.400
Hours= 87.0000
2002
122.900– 129.000
Hours= 146.000
ICME
2002
133.700– 136.200
Hours= 60.0000
2002
141.600– 146.000
Hours= 106.000
2002
159.500– 162.300
Hours= 67.0000
2002
166.000– 170.700
Hours= 113.000
ICME
2002
177.900– 181.300
Hours= 81.0000
2002
195.400– 197.400
Hours= 48.0000
2002
203.000– 205.500
Hours= 60.0000
2002
218.500– 221.700
Hours= 70.0000
2002
242.800– 247.200
Hours= 106.000
2002
266.400– 271.200
Hours= 113.000
2002
292.200– 298.300
Hours= 145.000
2002
320.700– 323.600
Hours= 69.0000
2002
339.100– 340.100
Hours= 24.0000
D. Lario

01-02

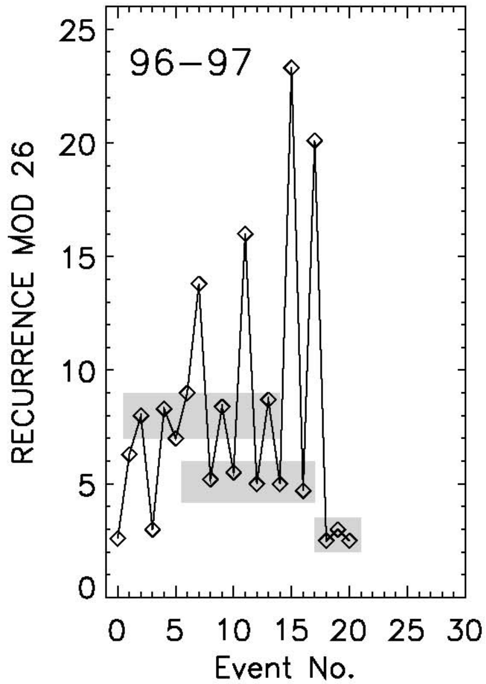

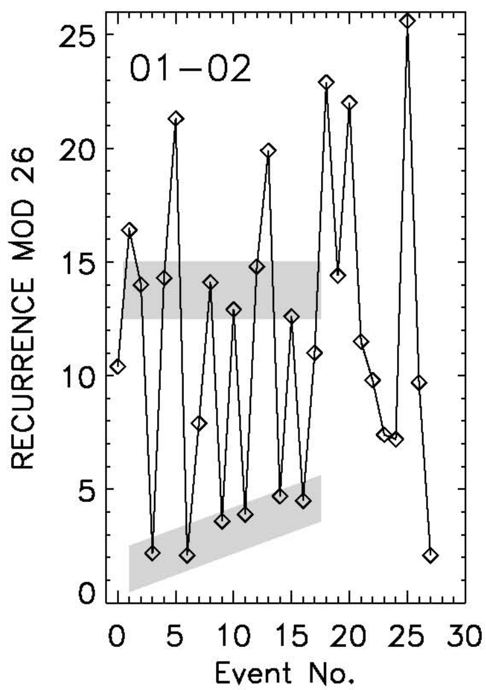

Search data for 26-day recurrent signatures:

Recurrent: most likely related to stable coronal holes

1996-7 (min):	6+5+3=14 out of 20	(70%)
2001-2 (max):	6+6=12 out of 27	(44%)

Non-recurrent: could be either transients in solar wind emission or short-lived coronal holes (at Ulysses latitudes)

1996-7 (min):	6 out of 20	(30%)
2001-2 (max):	15 out of 27	(56%)

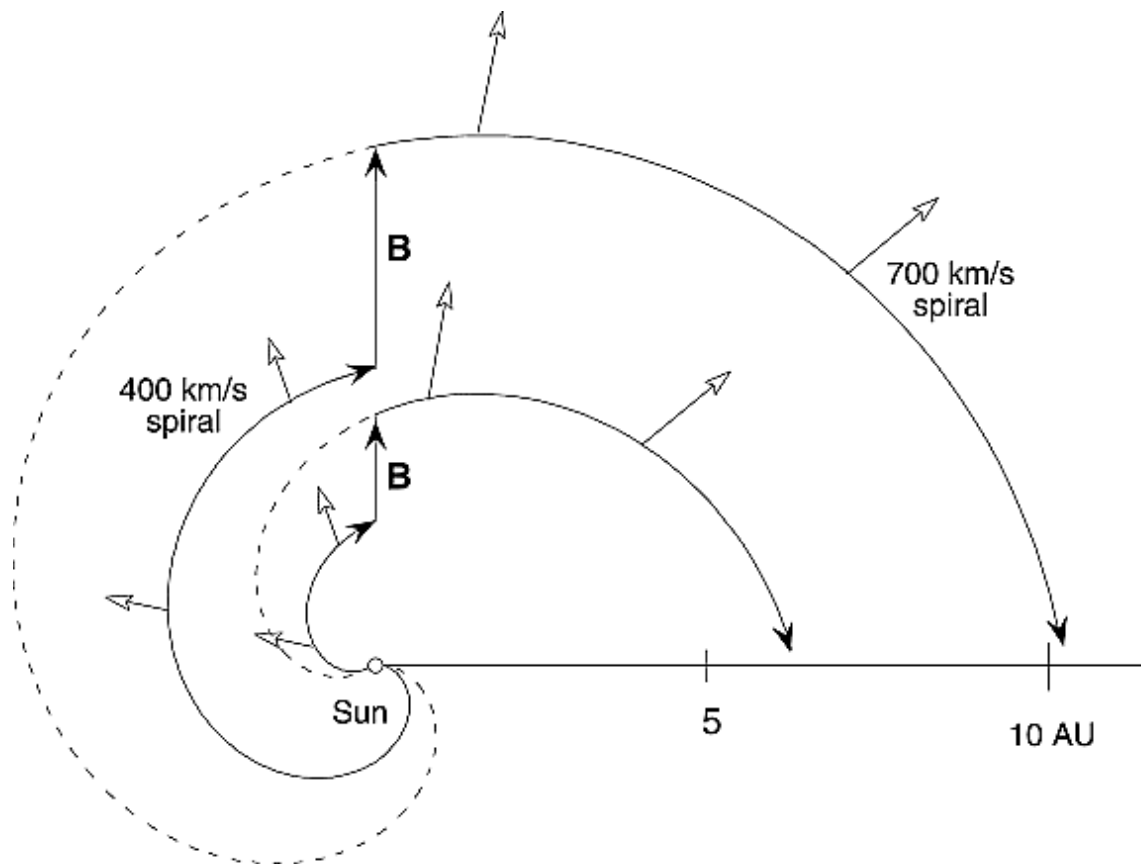

Gosling and Skoug [2002]

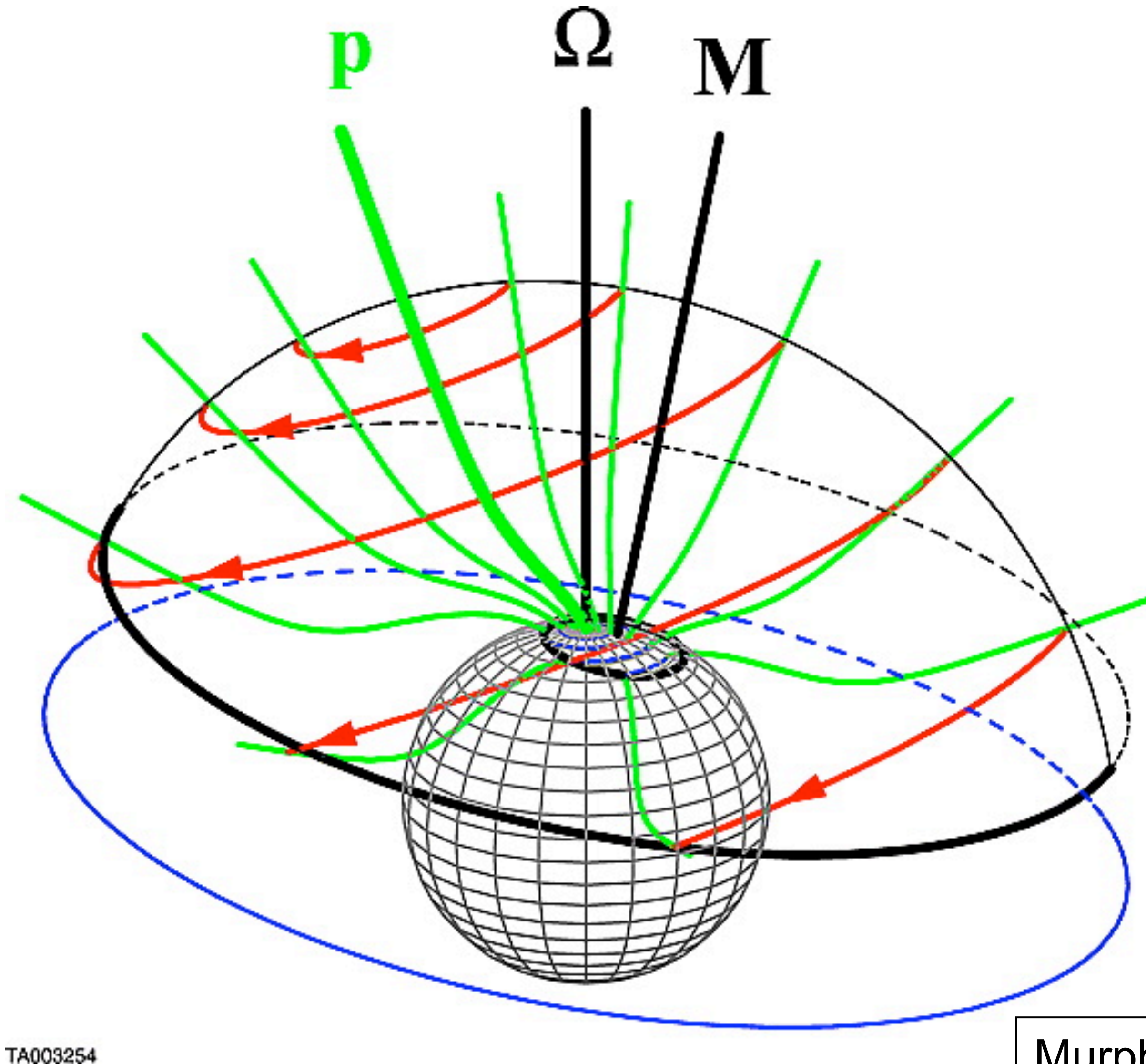

Murphy et al. [2002]

Schwadron [2002]

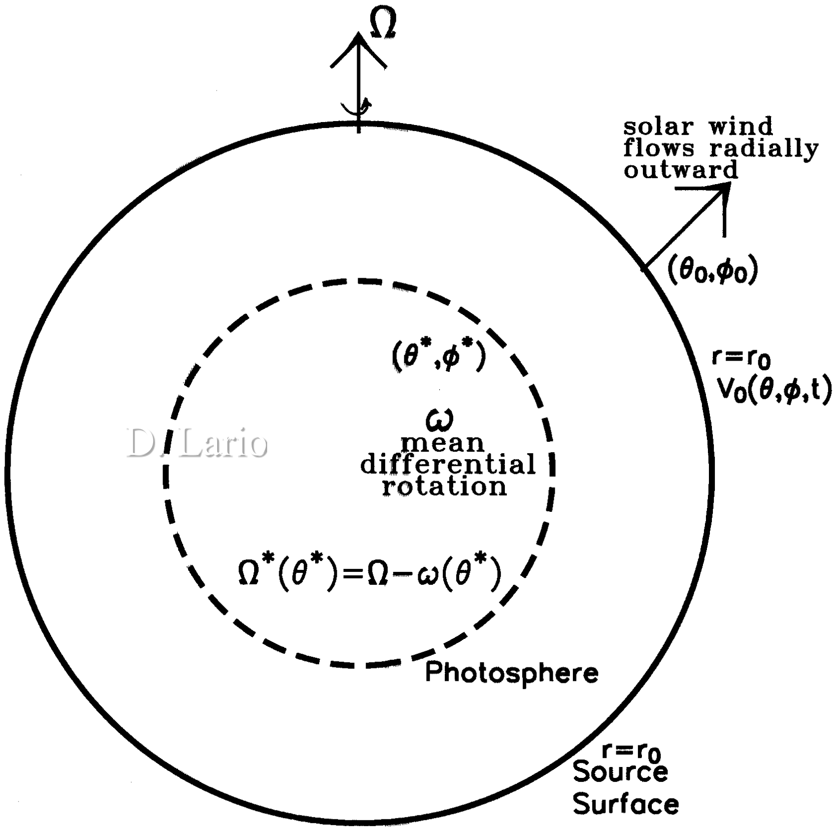

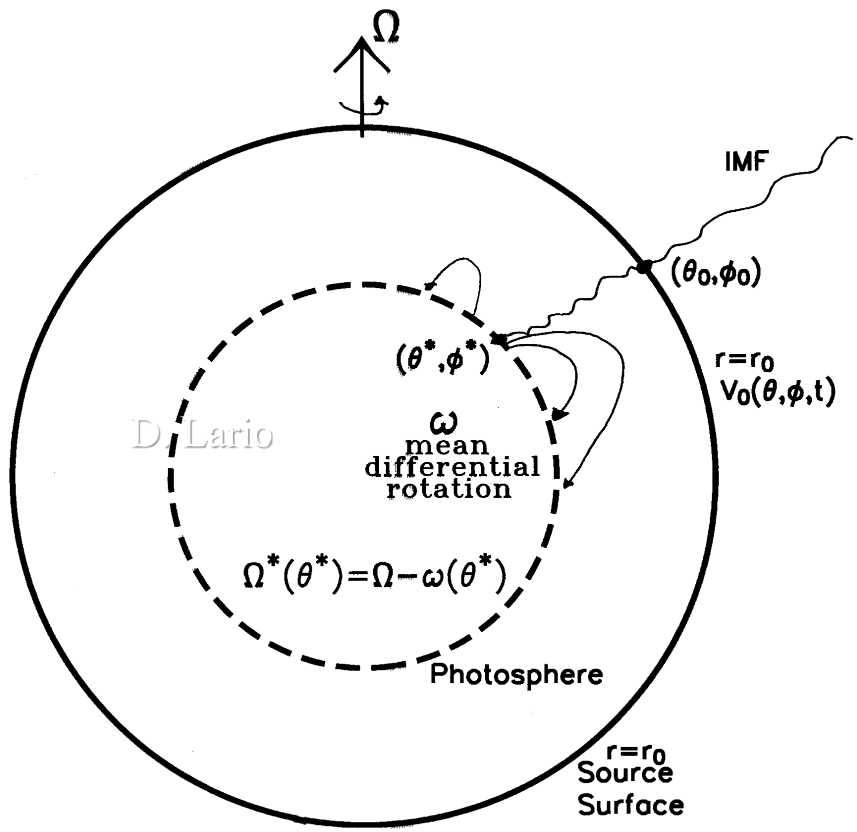

At the photosphere, we have the field lines rooted at θ^* and ϕ^*, and move with a mean angular velocity Ω^*, with

$$\Omega^*(\theta^*) = \Omega - \omega(\theta^*)$$

where ω is the mean differential angular velocity.

The parametric equations then simplify to

$$\left.\begin{array}{l} r = r_0 + \tau\, V_0\Big[\theta_0, \phi_0 + \omega(\theta_0)\tau, t - \tau\Big] \\ \theta = \theta_0 \\ \phi = \phi_0 + \omega(\theta_0)\tau - \Omega\tau = \phi_0 - \Omega^*(\theta_0)\tau \end{array}\right\}$$

From the last equation we have $\tau = (\phi_0 - \phi)/\Omega^*$, and replacing it in the first equation

$$r = r_0 + \frac{\phi_0 - \phi}{\Omega^*}\, V_0\Big[\theta_0,\ \phi_0 + \omega(\theta_0)\frac{\phi_0 - \phi}{\Omega^*},\ t - \frac{\phi_0 - \phi}{\Omega^*}\Big]$$

The function $V_0(\theta, \phi, t)$ is arbitrary.
The velocity itself $V(r, \theta, \phi, t)$ is assumed to be radial and ballistic and is defined as a function of position and time t, and we can define it in terms of the parameter τ

$$\left.\begin{array}{l} V = V_0(\theta,\ \phi + \Omega\tau, t - \tau) \\ r = r_0 + V\tau \end{array}\right\}$$

For a given values of the angular coordinates (θ, ϕ) and the time t, these equations generate V, at all distances $r > r_0$ with $0 < \tau < \infty$

$$V = V_0\Big(\theta,\ \phi + \Omega(\frac{r - r_0}{V}),\ t - \frac{r - r_0}{V}\Big)$$

The angle Ψ between the radial direction and the frozen-in magnetic field is

$$\tan\Psi = r\sin\theta/\left(\frac{dr}{d\phi}\right)$$

$$\frac{dr}{d\phi} = -\frac{V_0}{\Omega^*} + \frac{\phi_0-\phi}{\Omega^*}\left\{-\frac{\omega}{\Omega^*}\frac{\partial V_0}{\partial\phi} + \frac{1}{\Omega^*}\frac{\partial V_0}{\partial t}\right\}$$

$$\boxed{\tan\Psi = -\frac{(\Omega-\omega)r\sin\theta}{V_0 + \frac{\phi_0-\phi}{\Omega^*}[\omega\frac{\partial V_0}{\partial\phi} - \frac{\partial V_0}{\partial t}]}}$$

If $\frac{\partial V_0}{\partial t} = 0$

$$\tan\Psi = -\frac{(\Omega-\omega)r\sin\theta}{V_0 + \frac{\phi_0-\phi}{\Omega^*}[\omega\frac{\partial V_0}{\partial\phi}]}$$

Murphy et al. [2002].

If $\omega = 0$

$$\tan\Psi = -\frac{\Omega r\sin\theta}{V_0 - \frac{\phi_0-\phi}{\Omega}\frac{\partial V_0}{\partial t}}$$

Gosling and Skoug [2002]

Near-radial IMF in CIR rarefaction region

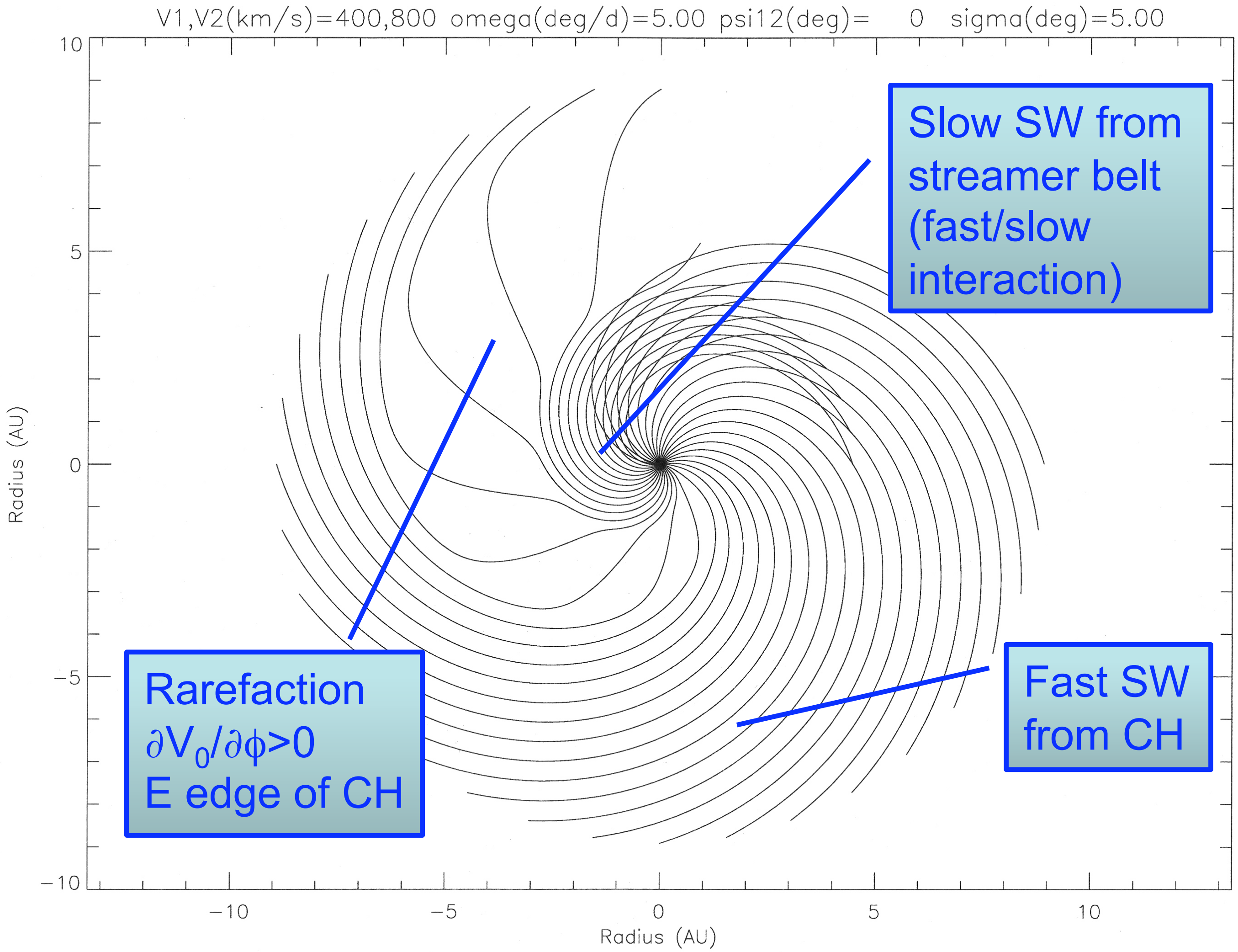

Propagation of energetic particles in rarefaction region from RS of CIR

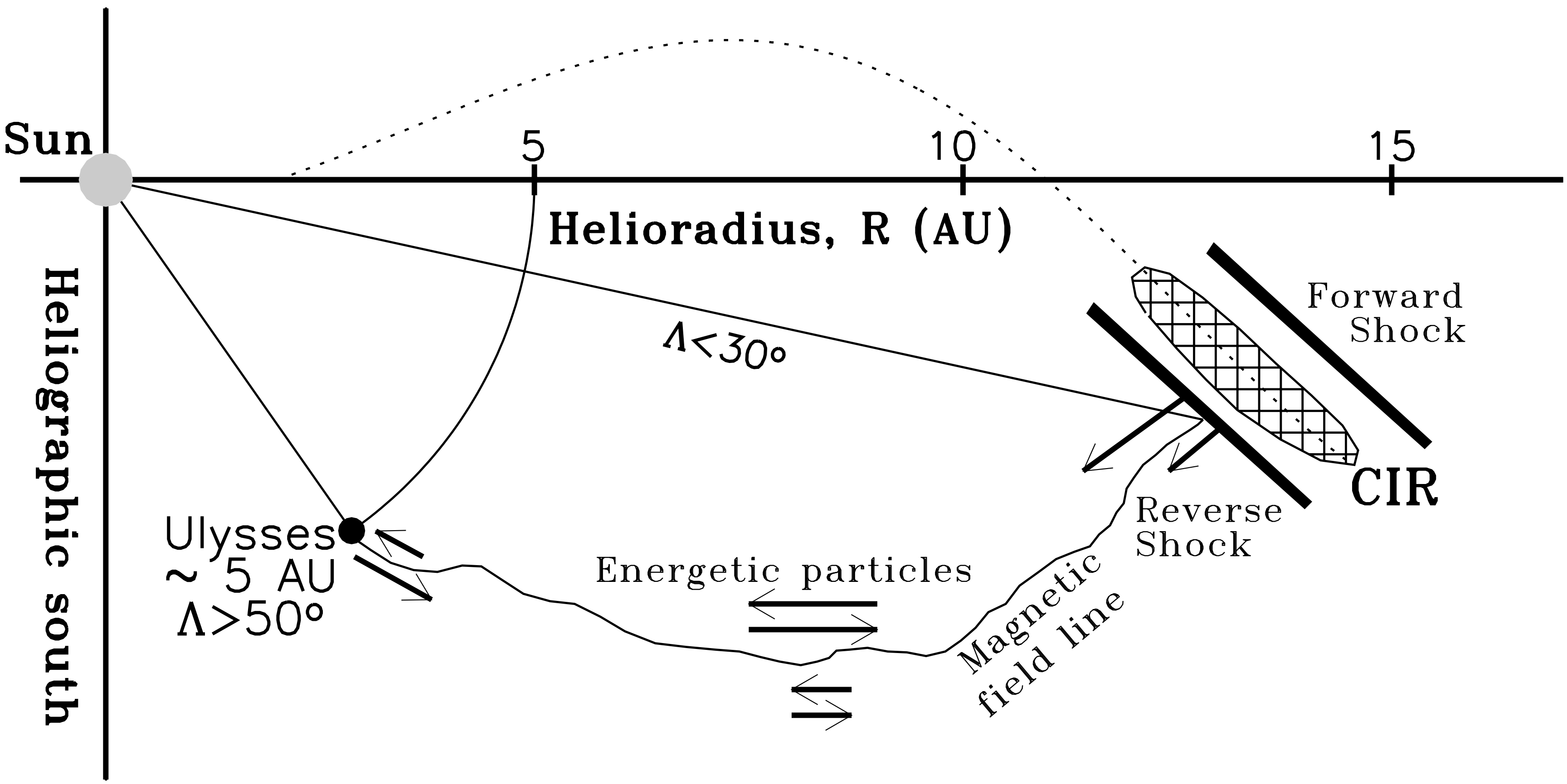

Simnett and Roelof [1995, 1999]; Roelof [2000]

Conclusions (1)

- Mid-latitude solar wind rarefaction regions:
  - coincide with "dwells" (solar wind originated at approximately the same longitude)
  - show low magnetic field magnitude
  - show non-Parker (more radial) magnetic field orientation
- 26-day recurrent series dominate outside of the solar maximum (92-93, 96-97, and part of 05-06).
- Non-recurrent rarefactions (including CMEs) are comparable to recurrent rarefactions during solar maximum (01-02):
  - a mix of coronal hole recurrences and transients either in the solar wind source or in the coronal hole evolution is observed.

Conclusions (2)

Implications for energetic particle propagation in rarefaction regions of CIRS:

When CIR plasma/field signatures are observed *in situ*, *e.g.* at 1AU, energetic particles are associated with both the forward and reverse shock (if formed).

For remote connection to CIRs, *e.g.,* Ulysses at mid and high latitudes, the IMF in rarefactions (that connects to the reverse shock is strongly deformed from an ideal Parker field (high probability of near-radial directions and very weak, quiet magnetic field).

These conditions are conducive to nearly scatter-free propagation of 0.06-5.0 MeV ions and 50-300 keV electrons from >15AU back into the inner heliosphere (1-5AU) *via* paths *much shorter* than the distance along a Parker spiral.

END

Thanks to the Organizing Committee!